Journal of Microbiology, Immunology and Infection 56 (2023) 853—862

Available online at www.sciencedirect.com

ScienceDirect

journal homepage: www.e-jmii.com

Original Article

The therapeutic effect of tanshinone IIA in mouse astrocytes after treatment with *Angiostrongylus cantonensis* fifth-stage larval excretory-secretory products

Kuang-Yao Chen [a,b,c,d,*], Yi-Ju Chen [d], Chien-Ju Cheng [a], Kai-Yuan Jhan [a], Cheng-Hsun Chiu [c], Lian-Chen Wang [a,b,c,]**

[a] *Department of Parasitology, College of Medicine, Chang Gung University, Taoyuan 333, Taiwan*
[b] *Graduate Institute of Biomedical Sciences, College of Medicine, Chang Gung University, Taoyuan 333, Taiwan*
[c] *Molecular Infectious Disease Research Center, Chang Gung Memorial Hospital, Taoyuan, Taiwan*
[d] *Department of Parasitology, School of Medicine, China Medical University, Taichung, 404, Taiwan*

Received 2 December 2022; received in revised form 30 March 2023; accepted 20 April 2023
Available online 25 April 2023

KEYWORDS
Angiostrongylus cantonensis;
Excretory-secretory products;
Tanshinone IIA;
Astrocytes

Abstract *Background: Angiostrongylus cantonensis* is an important food-borne zoonotic parasite that causes eosinophilic meningitis and meningoencephalitis in humans. Excretory-secretory products (ESPs) are valuable targets for studying host-parasite relationships. ESPs are composed of a variety of molecules that are used to penetrate defensive barriers and avoid immune attack of the host. Tanshinone IIA (TSIIA) is a vasoactive cardioprotective drug that is widely used in studies evaluating potential therapeutic mechanisms. In this study, we will evaluate the therapeutic effects of TSIIA in mouse astrocytes after *A. cantonensis* fifth-stage larvae (L5) ESPs treatment.
Methods: Here, we examined the therapeutic effect of TSIIA by real-time qPCR, western blotting, activity assay, and cell viability assays.
Results: First, the results showed that TSIIA can elevate cell viability in astrocytes after stimulation with ESPs. On the other hand, TSIIA downregulated the expression of apoptosis-related molecules. However, the expression of molecules related to antioxidant, autophagy, and endoplasmic reticulum stress was significantly increased. The results of antioxidant activation assays showed that the activities of superoxide dismutase (SOD), glutathione S-transferase

* Corresponding author. Department of Parasitology, College of Medicine, Chang Gung University, Taoyuan 333, Taiwan. Fax: +886 3 2218385.
** Corresponding author. Department of Parasitology, College of Medicine, Chang Gung University, Taoyuan 333, Taiwan. Fax: +886 3 2218385.
E-mail addresses: d000018229@cgu.edu.tw (K.-Y. Chen), wanglc@mail.cgu.edu.tw (L.-C. Wang).

https://doi.org/10.1016/j.jmii.2023.04.007

(GST), and catalase were significantly increased. Finally, we found that cell apoptosis and oxidative stress were reduced in TSIIA-treated astrocytes by immunofluorescence staining.
Conclusion: The findings from this study suggest that TSIIA can reduce cellular damage caused by *A. cantonensis* L5 ESPs in astrocytes and clarify the related molecular mechanisms.

Introduction

Excretory-secretory products (ESPs) from nematodes have many functions for parasitic helminths, such as migration and feeding and are also important targets in the study of interactions between parasitic nematodes and their hosts.[1] Previous studies have indicated that ESPs are important in parasite survival and development.[2–4] However, they also have the ability to modulate host immune responses, oxidative stress and host cell survival.[5]

Angiostrongylus cantonensis is an important food-borne zoonotic parasite that can cause severe neuropathological damage and symptoms, including eosinophilic meningitis and eosinophilic meningoencephalitis in humans.[6–11] In the clinic, the CNS symptoms of human angiostrongyliasis include severe headaches, fever, nausea, vomiting, neck stiffness, photophobia, blurred vision, and neurological abnormalities.

Tanshinone IIA (TSIIA) is an effective monomer component purified from the traditional Chinese medicinal herb Danshen (*Salvia miltiorrhiza*). In neurodegenerative disorder treatments, this compound can attenuate memory impairment by inhibiting cell apoptosis, inflammation, and amyloid peptide accumulation.[12–15] Moreover, many studies have also reported that TSIIA has protective functions for neurons in CNS injury and ischemic diseases.[16–23] Data from *A. cantonensis* infection studies showed that TSIIA can increase myelin sheath thickness and inhibit the expression of cytokines. These results indicated that TSIIA has therapeutic effects for angiostrongyliasis.[24]

Although TSIIA has been evaluated in many studies of cancers and neurodegenerative diseases, there are few studies about its therapeutic effect in pathogen infection, especially in parasitic nematode infection. The present study aims to evaluate the therapeutic efficiency of TSIIA after *A. cantonensis* L5 ESPs treatment. Moreover, we clarified the molecular mechanisms by which TSIIA mitigates ESPs-induced stress in astrocytes, including cell apoptosis, oxidative stress, autophagy, and ER stress. This study is the first to evaluate the protective function of TSIIA treatment on central nervous system-related cells after stimulation with the ESPs of fifth-stage *A. cantonensis* larvae.

Methods

A. cantonensis infection and excretory/secretory product collection

In this study, the strain of *A. cantonensis* has been maintained in our laboratory since 1985. This strain was isolated from an *Achatina fulica* snail collected in Taipei. A total of 200 *A. cantonensis* L3 were used to infect Sprague–Dawley rats (SD rats) by stomach intubation using a feeding tube. After completely anesthetized with 3% (v/v) isoflurane (Panion & BF Biotech Inc., Taipei, Taiwan), blood samples are collected by cardiac puncture and the L5 were then isolated from the brain tissues at days 25 post-infection. By determining the reproductive organ development at the tail of worms, it can be confirmed that it is the L5. After washing with saline, phosphate buffered saline, and RPMI (Sigma–Aldrich, USA), the worms were incubated in Gibco Roswell Park Memorial Institute (RPMI) medium without fetal bovine serum (FBS). The ESPs of L5 were collected from the cultured medium and concentrated using an Amicon Ultra-15 10 K centrifugal filter device (Merck Millipore, Germany).

All animal procedures in this study were approved by the Chang Gung University Institutional Animal Care and Use Committee (IACUC) in Taiwan (CGU110-231) and followed the guideline for Laboratory Animal Facilities and Care (The Council of Agriculture. Executive Yuan, ROC). Rats and mice were housed in plastic cages and provided with food and water ad libitum. The experimental animals were sacrificed by anesthesia with isoflurane (1 ml/min).

Cell culture and tanshinone IIA treatment

Mouse astrocytes (CRL2535) were cultured in culture flasks containing Dulbecco's modified Eagle's medium/F-12 (DMEM/F-12) (Corning, USA), 10% fetal bovine serum (FBS) (Gibco, USA), and penicillin and streptomycin. Cells were plated and incubated onto culture dishes with serum-free DMEM/F-12 for 24 h. Finally, cells were pretreated with tanshinone IIA (TSIIA) for 2 h. Next, the 250 or 500 μg/ml A. *cantonensis* L5 ESPs were used to treat cells for 12 h (C: Control; E250: 250 μg/ml ESPs; E500: 500 μg/ml ESPs; T3: 250 μg/ml ESPs+3 μg/ml TSIIA; T6: 250 μg/ml ESPs+6 μg/ml TSIIA; T12: 250 μg/ml ESPs+12 μg/ml TSIIA; T25: 250 μg/ml ESPs+25 μg/ml TSIIA).

Cell viability assay

The astrocytes (1×10^7 cells/ml) were collected after ESPs or TSIIA (3, 6, 12.5, and 25 μg/ml) treatment and incubated with CCK-8 (Cell Counting Kit-8) (Sigma–Aldrich, USA) at 37 °C in the dark with mild shaking for 1 h. Cell survival was monitored by measuring formazan dye absorbance at 450 nm using a spectrophotometer (Molecular Devices, USA).

RNA extraction and RNA-sequencing library

Total RNA of astrocytes in different treatment conditions, including ESPs and drugs, was extracted. TRIzol® reagents were used to purify total RNA from the different treatment groups. The TruSeq Stranded mRNA Library Prep Kit (Illumina, San Diego, CA, USA) was employed to prepare the purified RNA before sequencing. Finally, the qualified libraries were sequenced on an Illumina NovaSeq 6000 platform with 150 bp paired-end reads generated by Genomics, BioSci & Tech Co., New Taipei City, Taiwan.

Quantitative real-time PCR (qRT–PCR)

In this study, cDNA synthesis and qRT–PCR were carried out using an iScript™ cDNA Synthesis Kit and an iQ™ SYBR® Green Supermix kit (Bio-Rad, USA). The 20 μl PCR mixture contained 1 μg reverse transcription product, master mix, and 0.5 μM real-time forward and reverse primers. BIO-RAD CFX Connect was used to detect gene expression in astrocytes.

Protein extraction and Western blotting

The total protein of astrocytes was extracted in lysis buffer containing protease inhibitors (Roche Diagnostics, Switzerland). Next, the proteins were separated by 12% SDS–PAGE and transferred to nitrocellulose membranes. The membranes were incubated with antibodies against Bax (ABclonal, USA), Bid (ABclonal, USA), Caspase-3 (ABclonal, USA), Bcl-2 (ABclonal, USA), p53 (ABclonal, USA), superoxide dismutase (ABclonal, USA), glutathione transferase kappa (ABclonal, USA), LC3b (ABclonal, USA), Beclin-1 (ABclonal, USA), GRP78 (Proteintech, USA), ATF4 (Signalway Antibody, USA), ATF6 (Proteintech, USA), and β-actin (Proteintech, USA). The membranes were incubated with HRP-linked secondary antibody (Sigma–Aldrich, USA). Finally, the immunoreactive bands were detected by ECL reagent (EMD Millipore, USA) and a ChemiDoc Imaging System (Bio-Rad, USA).

Antioxidant capacity assay

The cell lysate was collected from astrocytes after ESP or TSIIA treatment. Metmyoglobin, chromogen, and hydrogen peroxide were added to detect the antioxidant capacity (Cayman, USA) by reading the absorbance at 405 nm using a spectrofluorometer (Molecular Devices, USA).

Antioxidant activity assay

A catalase assay kit was used to detect catalase activity in astrocytes (Cayman, USA). Add Catalase Potassium Hydroxide, Catalase Hydrogen Peroxide, Catalase Purpald, and Catalase Potassium Periodate into each well of both samples and controls to start the reaction. Measure the absorbance at 540 nm using a spectrofluorometer. A SOD determination kit detected SOD activity in astrocytes (Cayman, USA). Add 20 μl of sample solution to each sample, and add ddH_2O to each blank well. Add WST Working Solution to each well, and mix. Add Enzyme Working Solution to each sample and incubate the plate at 37 °C for 20 min. Read the absorbance at 450 nm using a microplate reader. A Glutathione S-Transferase (GST) determination kit detected GST activity in astrocytes (Cayman, USA). Add sample solution to each sample, and add ddH_2O to each blank well. Add Glutathione to each well, and mix. Add CDNB to each sample. Read the absorbance at 340 nm using a microplate reader.

ROS detection assay

ROS generation in astrocytes was detected using a Reactive oxygen species (ROS) detection assay kit (Cayman, USA) according to the manufacturer's instructions. ROS are highly reactive chemicals, such as hydroxyl radicals, peroxides, and superoxide. The astrocytes were incubated with Dihydroethidium assay reagent, Antimycin A assay reagent, and N-acetyl Cysteine assay reagent. Finally, ROS production was detected by a fluorescent microscope.

Cell apoptosis assay

Cell apoptosis in astrocytes was detected using a cell apoptosis kit (Cayman, USA) according to the manufacturer's instructions. The cells were collected and washed twice with cold PBS, incubated with Apopxin Green Indicator, AAD, and CytoCalcein Violet450 for 40 min at room temperature, and then detected by a fluorescent microscope.

Statistical analysis

Statistical analysis was performed using GraphPad Prism 5 software (GraphPad, USA), and data are presented as the mean ± SD. Differences between groups were compared by Student's t test. $P < 0.05$, < 0.01, and < 0.001 were considered statistically significant.

Results

The effect of TSIIA on the survival rate of astrocytes after treatment with *A. cantonensis* L5 ESPs

To evaluate the protective efficiency of TSIIA in astrocytes after treatment with *A. cantonensis* L5 ESPs, cells were pretreated with different concentrations of TSIIA (3, 6, 12.5, and 25 μg/ml) for 2 h. Next, the 250 or 500 μg/ml A. *cantonensis* L5 ESPs were used to treat cells for 12 h. Cell viability was observed by the CCK8 assay (Fig. 1). The results showed that ESPs induced cell death in astrocytes. Conversely, the cell viability percentage was significantly increased after TSIIA treatment. Therefore, the data suggested that TSIIA has protective efficiency in astrocytes after treatment with *A. cantonensis* L5 ESPs.

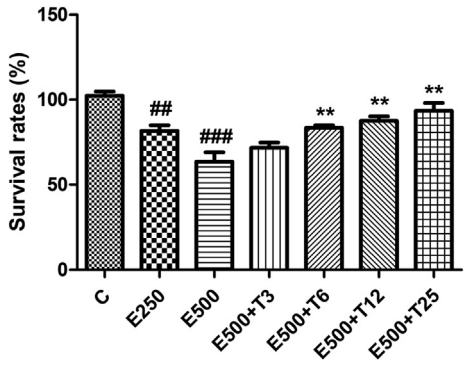

Figure 1. Effect of tanshinone IIA on the survival rate of astrocytes treated with the excretory/secretory products of *A. cantonensis* L5. Cells were pretreated with tanshinone IIA (TSIIA) and then incubated with *A. cantonensis* L5 excretory/secretory products (ESPs). Cell viability of astrocytes was analyzed by the CCK-8 assay. The data are expressed as the means ± SDs from three independent experiments (n = 3). $^{\#\#}P < 0.01$, $^{\#\#\#}P < 0.001$, compared to control. $^{**}P < 0.01$, compared to cells exposed to 500 μg/ml ESPs.

Characteristics of the transcriptome of astrocytes after *A. cantonensis* L5 ESPs and TSIIA treatment

We initially employed next-generation sequencing (NGS) to establish RNA-seq profiling for astrocytes in different treatment groups. We set up three databases containing the data of the Control, ESPs, ESPs + 12.5 μg/ml TSIIA, and ESPs + 25 μg/ml TSIIA treatment groups. Approximately 204,006,000 Uniq reads and 29,420,000,000 Uniq bases (bp) were obtained (Table 1). A Venn diagram was used to show the number of differentially expressed genes in each comparison by RSEM and EBSeq (PPEE ≤ 0.05) (Fig. 2A). A total of 123 genes were identified as differentially expressed genes (DEGs) in the E/N and T/E groups, and 4699 genes are shown in the union of comparisons. Finally, we detected the expression of the DEGs in terms of transcripts per million (TPM) in each group (Fig. 2B). The results showed that TSIIA reduced the expression of cell apoptosis-related genes and increased the expression of oxidative stress-, autophagy-, and endoplasmic reticulum stress-related genes after *A. cantonensis* L5 ESPs treatment.

Effect of pretreatment of TSIIA on cell apoptosis induction in *A. cantonensis* L5 ESPs stimulated astrocytes

To determine the effect of TSIIA on cell apoptosis in astrocytes, we investigated whether TSIIA could reduce ESPs-induced cell apoptosis. The western blotting data showed that the protein expression of cell apoptosis-related molecules, such as Bax, Bid, Caspase-3, Bcl-2, and p53, was significantly elevated after ESPs treatment. However, TSIIA reduced cell apoptosis-related protein expression after ESPs treatment (Fig. 3A). The gene expression levels also showed the same results (Fig. 3B). Finally, the fluorescence staining results also demonstrated that the expression of cell apoptosis-related genes (membrane PS, green color) was significantly lower in the cells pretreated with TSIIA (12.5 and 25 μg/ml) than in those treated with ESPs alone (Fig. 3C). These results demonstrated that TSIIA can reduce cell apoptosis in astrocytes after treatment with *A. cantonensis* L5 ESPs.

Effect of pretreatment of TSIIA on oxidative stress generation in *A. cantonensis* L5 ESPs stimulated astrocytes

To evaluate the effect of TSIIA on oxidative stress in astrocytes, we investigated whether TSIIA could reduce oxidative stress. The western blotting data showed that the protein expression of antioxidants (GSTK1 and SOD) was increased after ESPs treatment. However, TSIIA elevated antioxidant expression after ESPs treatment (Fig. 4A). The gene expression levels also showed the same results (Fig. 4B). The fluorescence staining results also demonstrated that ROS expression (green color) was significantly lower in the cells pretreated with TSIIA (12.5 and 25 μg/ml) than in those treated with ESPs alone (Fig. 4C). Next, we also found that the antioxidant capacity was significantly higher in the cells pretreated with TSIIA (12.5 and 25 μg/ml) than in those treated with ESPs alone (Fig. 4D). Finally, we monitored the activity of antioxidants, such as catalase, GST, and SOD, in astrocytes after *A. cantonensis* L5 ESPs or TSIIA treatment. The data showed that TSIIA induced antioxidant activation after ESPs treatment (Fig. 5). These

Table 1 Cleaned FASTQ Files Summary

Name	GC.	Length	Length_Mean	Phred	Q20_Ratio	Q30_Ratio	Qual_Mean	Read_Counts	Total_Bases
C-R1	48.65%	20—151	144.32	33	99.04%	96.29%	36.42	2,59,20,999	3,74,08,44,537
C-R2	48.78%	20—151	143.69	33	98.43%	94.35%	36.1	2,59,20,999	3,72,45,77,535
E-R1	48.00%	20—151	144.66	33	98.97%	96.05%	36.38	2,36,17,944	3,41,65,35,104
E-R2	48.22%	20—151	144.22	33	98.61%	94.87%	36.19	2,36,17,944	3,40,61,83,730
T12_R1	49.11%	20—151	144.65	33	99.05%	96.37%	36.43	2,62,17,641	3,79,22,92,916
T12_R2	49.28%	20—151	143.91	33	98.38%	94.29%	36.09	2,62,17,641	3,77,30,42,137
T25_R1	49.47%	20—151	144.43	33	99.03%	96.28%	36.42	2,62,49,842	3,79,12,11,118
T25_R2	49.62%	20—151	143.93	33	98.50%	94.61%	36.14	2,62,49,842	3,77,80,21,599

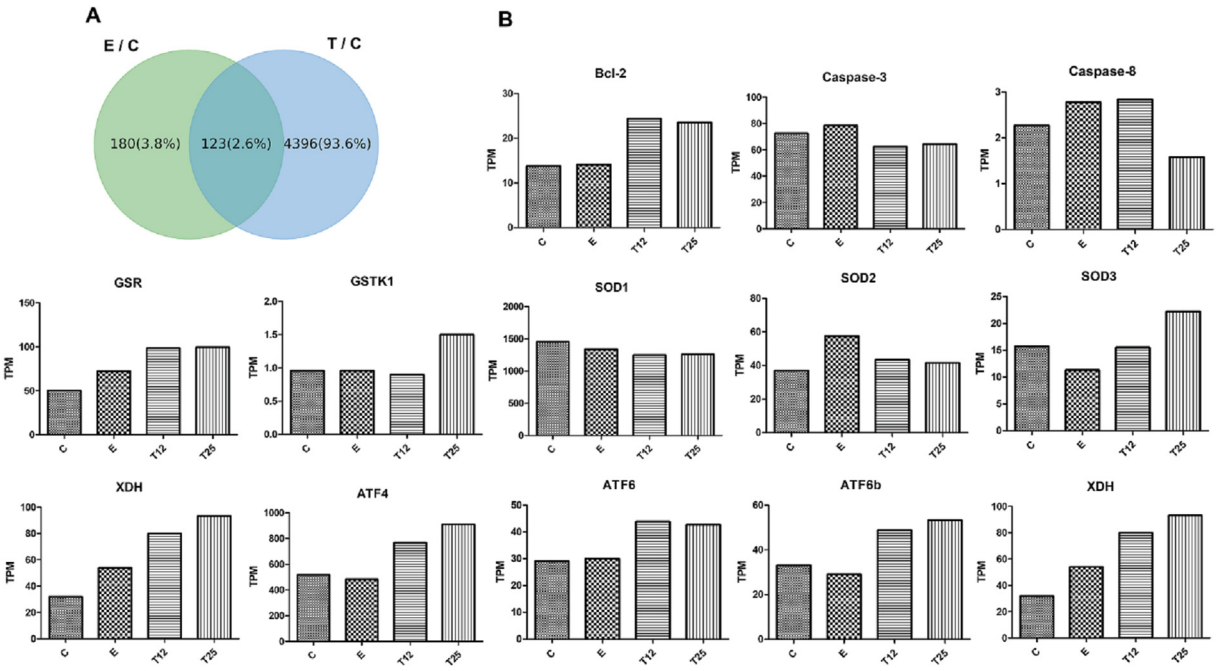

Figure 2. Summary of the RNA-seq and gene expression data (A) Venn diagram showing the number of differentially expressed genes in each comparison as determined by RSEM and EBSeq (PPEE ≤ 0.05) (B) The expression in TPM (transcripts per million) of the Control, ESPs, ESPs + 12.5 μg/ml TSIIA, and ESPs + 25 μg/ml TSIIA groups (E/C: ESPs group compared with Control group; T/C: ESPs+25 μg/ml TSIIA group compared with ESPs group).

results demonstrated that TSIIA can reduce oxidative stress in astrocytes after treatment with *A. cantonensis* L5 ESPs.

Effect of pretreatment of TSIIA on autophagy generation in *A. cantonensis* L5 ESPs stimulated astrocytes

Next, we investigated whether TSIIA could induce autophagy. The western blotting data showed that the protein expression levels of autophagy-related molecules, such as LC3b and Beclin-1, were significantly elevated after ESPs treatment. Moreover, TSIIA further elevated the expression of autophagy-related molecules after ESPs treatment (Fig. 6A). The gene expression levels also showed the same results (Fig. 6B). These results demonstrated that TSIIA can induce autophagy in astrocytes after treatment with *A. cantonensis* L5 ESPs.

Effect of pretreatment of TSIIA on endoplasmic reticulum stress generation in *A. cantonensis* L5 ESPs stimulated astrocytes

Finally, we wanted to determine whether TSIIA could induce endoplasmic reticulum (ER) stress. The western blotting data showed that the protein expression levels of ER stress-related molecules, such as GRP78, ATF4, ATF6, and PERK, were significantly elevated after ESPs treatment. Moreover, TSIIA elevated the expression of ER stress-related molecules after ESPs treatment (Fig. 7A). The gene expression levels also showed the same results (Fig. 7B). These results demonstrated that TSIIA can induce ER stress in astrocytes after treatment with *A. cantonensis* L5 ESPs.

Discussion

Astrocytes, glial cells, are the most abundant cells in the human CNS. They can secrete regulatory proteins or cytokines to control neuron activation and immune responses in pathogen infection.[25] Activated astrocytes generate TNF-α, IL-1β and IL-6 extracellularly and reduce neuronal death under oxidative stress.[26] These cells can form the blood–brain barrier (BBB) with endothelial cells and interact with neurons and blood vessels.[27,28]

In pathogen infection or stress stimulation, astrocytes can control neuronal activation and immune responses through secretion of regulatory proteins or cytokines.[29] In our previous studies, we first demonstrated that oxidative stress and cell apoptosis were induced in astrocytes by *A. cantonensis* L5 ESPs treatment.[6] In contrast, we also found that *A. cantonensis* ESPs can stimulate autophagosome formation and endoplasmic reticulum (ER) stress in astrocytes.[30,31] In a host immune response study, we found that NF-κB can stimulate cytokine secretion through the Shh signaling pathway in ESP-treated astrocytes.[32] In this study, the results showed that TSIIA has protective effects on astrocytes by reducing cell death after *A. cantonensis* L5 ESPs treatment.

Recently, administration of albendazole in combination with immunosuppressive drugs, such as corticosteroids,[33,34] schisandrin B,[35] and tanshinone IIA, was shown to possibly be a favorable treatment strategy for angiostrongyliasis.[23,36] However, our previous studies showed that

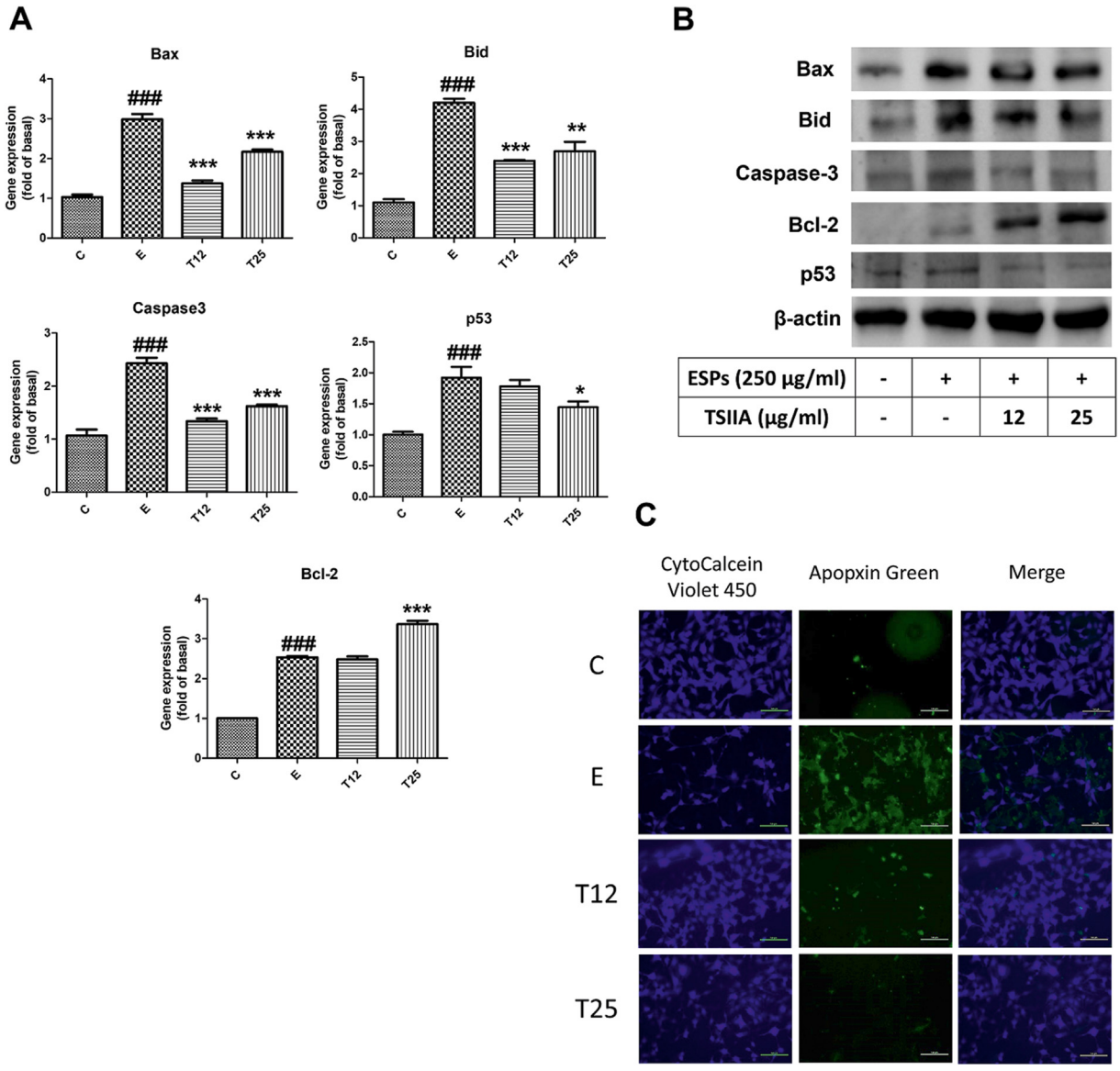

Figure 3. Tanshinone IIA reduced cell apoptosis in astrocytes after treatment with excretory/secretory products of *A. cantonensis* L5. Cells were pretreated with tanshinone IIA (TSIIA)and then incubated with *A. cantonensis* L5 excretory/secretory products (ESPs). The (A) mRNA and (B) protein expression levels were detected. The data are expressed as the means ± SD from three independent experiments (n = 3). $^{###}P < 0.001$, compared to control. $^{*}P < 0.05$, $^{**}P < 0.01$, and $^{***}P < 0.001$, compared to cells exposed to ESPs (C) An apoptosis/necrosis assay kit was used to detect cell apoptosis by fluorescence microscopy (n = 3). Scale bar = 100 μm.

administration of corticosteroids alone cannot directly attenuate *A. cantonensis*-induced brain damage.[37] To improve the treatment quality for human angiostrongyliasis, using other anthelmintics or immunosuppressive drugs with few side effects may be a potential therapeutic strategy. Finally, a previous study found that TSIIA combined with albendazole can protect the optic nerve by inhibiting the inflammation caused by *A. cantonensis* infection.[36]

In this study, we initially used NGS to establish RNA-seq profiling for astrocytes in different treatment groups. We found that TSIIA can downregulate the expression of cell apoptosis-related genes and elevate the expression of oxidative stress-, autophagy-, and endoplasmic reticulum stress-related genes after *A. cantonensis* L5 ESPs treatment. Finally, the western blotting results confirmed these expression changes in protein levels.

First, the results showed that the excretory/secretory products of *A. cantonensis* L5 can stimulate cell apoptosis in astrocytes and that tanshinone IIA (TSIIA) has a therapeutic effect via inhibition of cell apoptosis. Apoptosis is an active planned cell death pathway that is usually caused by physiological or pathological factors. During apoptosis, the cells initially shrink, and the DNA is degraded to 180—200 bp fragments by endonucleases. Some studies have demonstrated that TSIIA in combination with cyclosporine A (CsA) may inhibit myocardial cell apoptosis caused by renal ischemia and reperfusion in obese rats. Furthermore, TSIIA

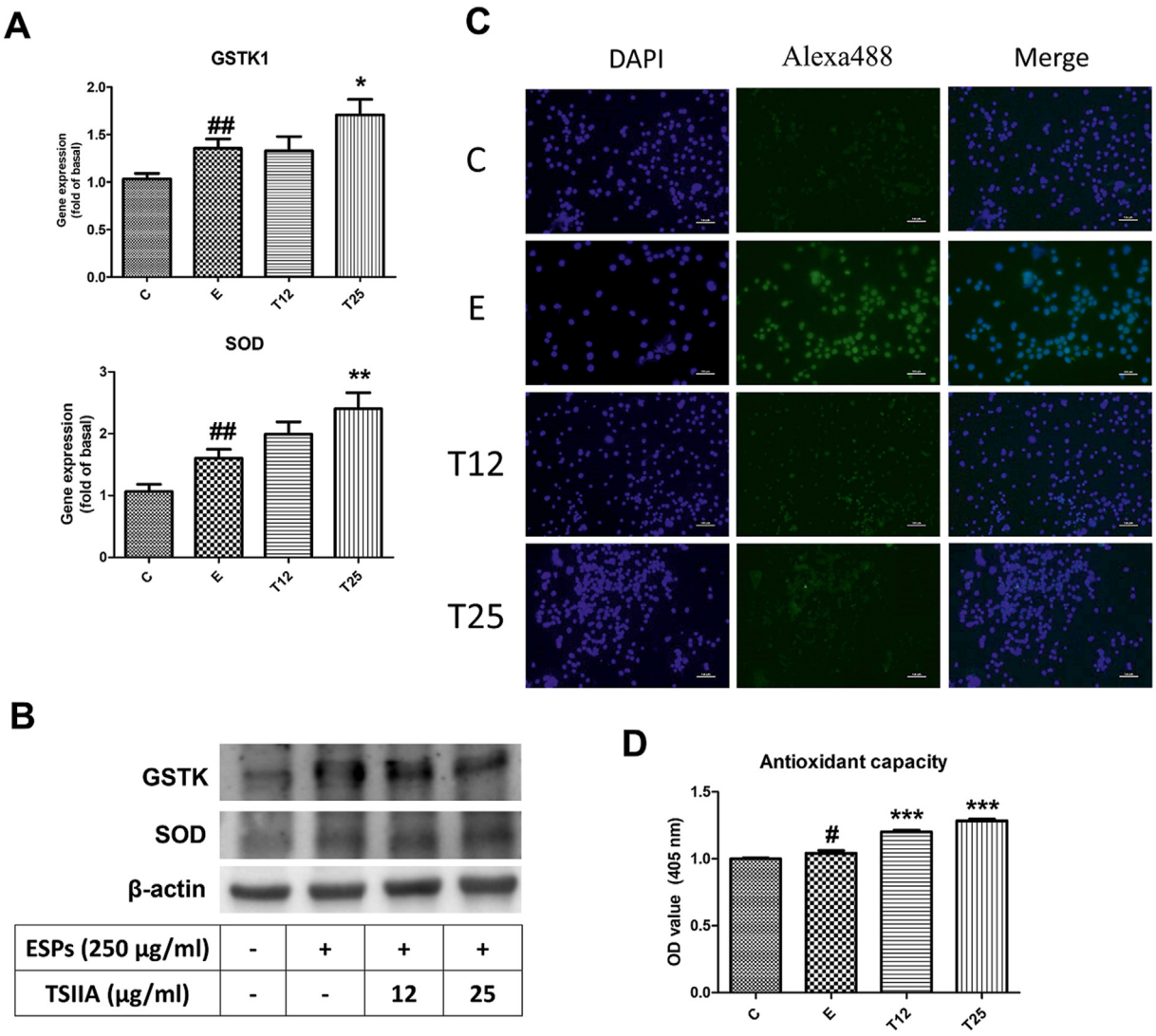

Figure 4. Tanshinone IIA reduced oxidative stress in astrocytes after treatment with excretory/secretory products of *A. cantonensis* L5. Cells were pretreated with tanshinone IIA (TSIIA) and then incubated with*A. cantonensis* L5 excretory/secretory products (ESPs). The (A) mRNA and (B) protein expression levels were detected. The data are expressed as the means ± SDs from three independent experiments (n = 3). $^{\#\#}P < 0.01$, compared to control. $^{*}P < 0.05$, and $^{**}P < 0.01$, compared to cells exposed to ESPs (C) An ROS detection cell-based assay was used to detect ROS generation by fluorescence microscopy (n = 3). Scale bar = 100 μm (D) An antioxidant assay kit was employed to detect antioxidant capacities in astrocytes (n = 3). $^{\#}P < 0.05$, compared to control. $^{***}P < 0.001$, compared to cells exposed to ESPs.

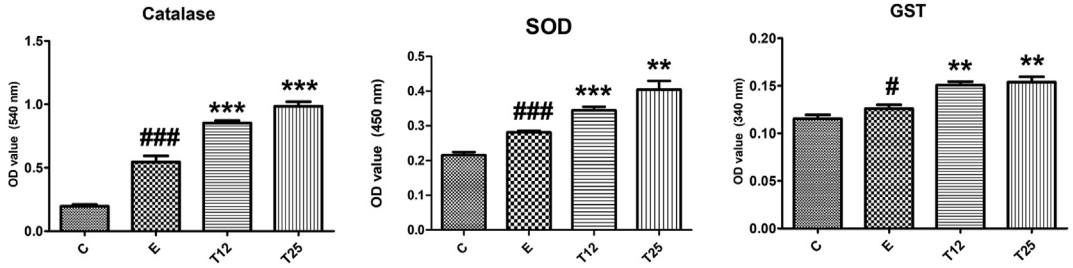

Figure 5. Tanshinone IIA induced antioxidant activation in astrocytes after treatment with excretory/secretory products of *A. cantonensis* L5. Cells were pretreated with tanshinone IIA (TSIIA and then incubated with *A. cantonensis* L5 excretory/secretory products (ESPs). The activities of catalase, SOD, and GST were determined by an activity assay (n = 3). $^{\#}p < 0.05$, $^{\#\#\#}p < 0.001$, compared to control.

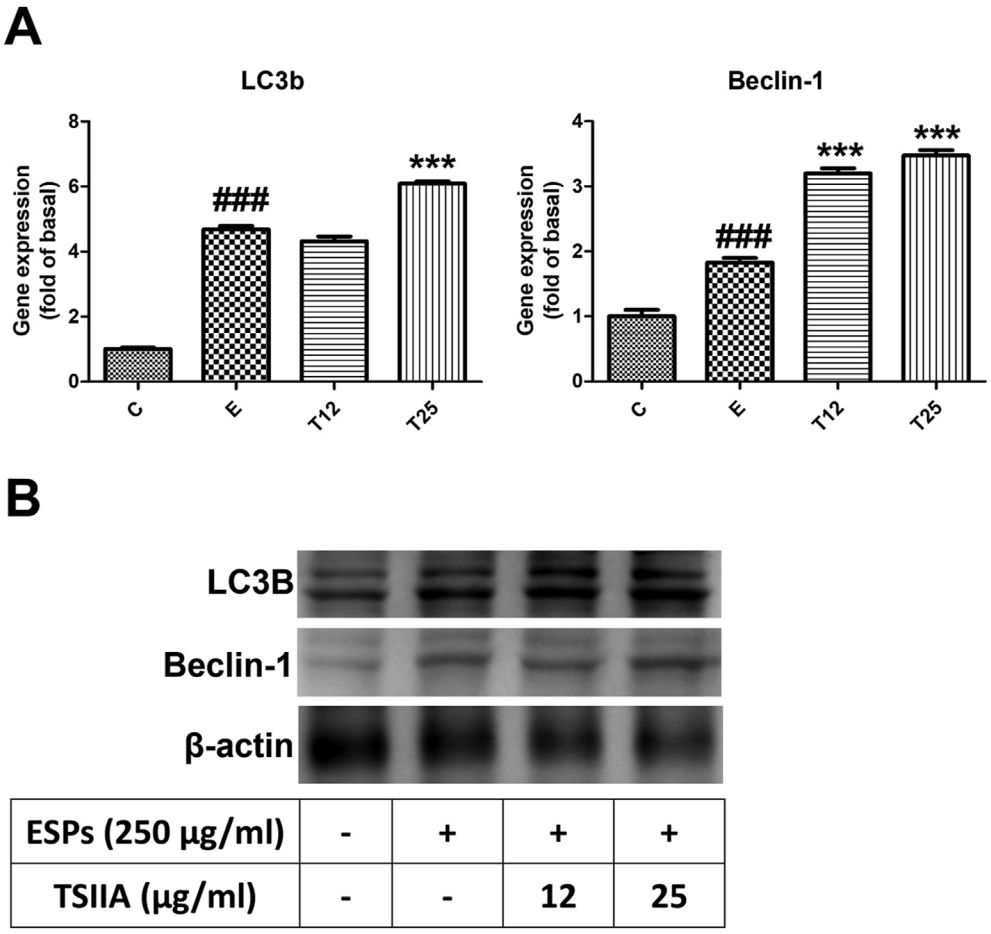

Figure 6. Tanshinone IIA induced autophagy in astrocytes after treatment with excretory/secretory products of *A. cantonensis* L5. Cells were pretreated with tanshinone IIA (TSIIA) and then incubated with *A. cantonensis* L5 excretory/secretory products (ESPs). The (A) mRNA and (B) protein expression levels were detected. The data are expressed as the means ± SD from three independent experiments (n = 3). $^{###}P < 0.001$, compared to control. $^{***}P < 0.001$, compared to cells exposed to ESPs.

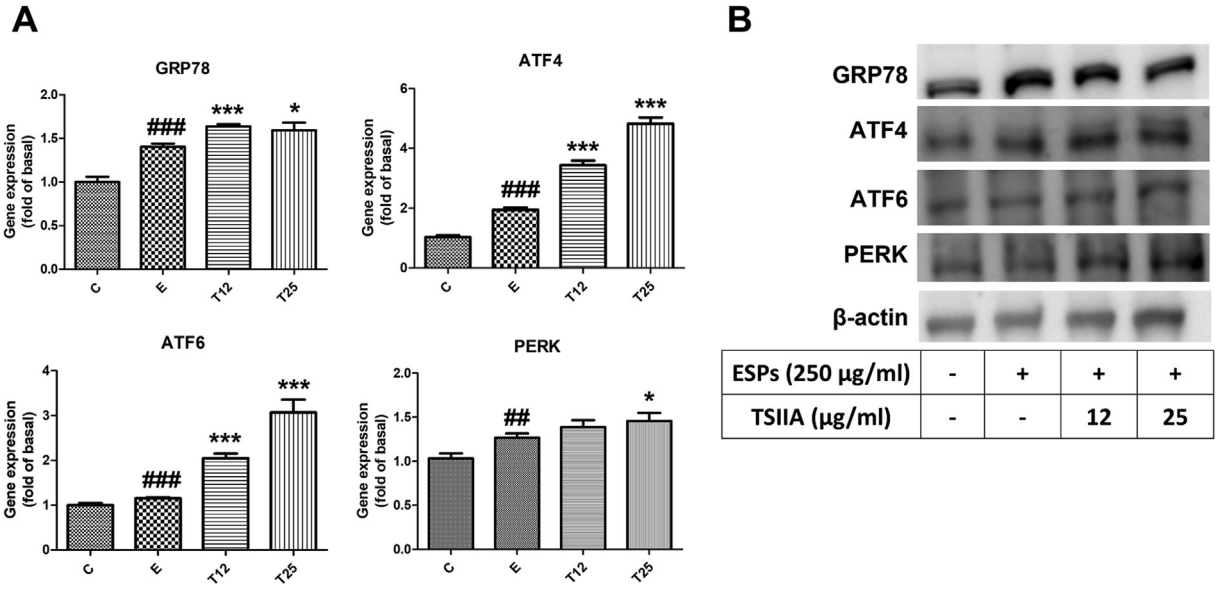

Figure 7. Tanshinone IIA induced ER stress in astrocytes after treatment with excretory/secretory products of *A. cantonensis* L5. Cells were pretreated with tanshinone IIA (TSIIA) and then incubated with *A. cantonensis* L5 excretory/secretory products (ESPs). The (A) mRNA and (B) protein expression levels were detected. The data are expressed as the means ± SD from three independent experiments (n = 3). $^{##}P < 0.01$, and $^{###}P < 0.001$, compared to control. $^{*}P < 0.05$ and $^{***}P < 0.001$, compared to cells exposed to ESPs.

combined with CsA treatment has been shown to attenuate renal IR-induced cardiomyocyte apoptosis in obese rats by activating the PI3K/Akt/Bad signaling pathway.[38]

Oxidative stress is a series of adaptive responses caused by the imbalance between reactive oxygen species and antioxidant mechanisms. This stress can damage proteins, lipids, and DNA by generating peroxides and free radicals. Oxidative stress in humans is thought to be responsible for cancer, Alzheimer's disease, Parkinson's disease, heart failure, atherosclerosis, attention deficit hyperactivity disorder and Asperger's syndrome.[39,40] However, oxidative stress also has benefits that the immune system uses to attack and kill pathogens; short-term oxidative stress plays an important role in preventing aging. Previous studies have shown that TSIIA can improve cardiac dysfunction and fibrosis by inhibiting oxidative stress.[41] The results demonstrated that TSIIA increases the expression of collagen I, collagen III, TGF-β, α-smooth muscle actin (α-SMA), matrix metalloproteinase 2 (MMP2) and MMP9 and regulates the activities of superoxide dismutase, malondialdehyde, and NADPH oxidase (Nox). In this study, we found that TSIIA reduced oxidative stress in astrocytes after treatment with *A. cantonensis* L5 ESPs.

In our Benzaldehyde research, our data found that the expression of apoptosis-related molecules was increased in response to *A. cantonensis* L5 s ESPs treatment. However, the cell viability of astrocytes was elevated by treating with 3-HBA and 4-HBA. Further investigation found that 3-HBA and 4-HBA can inhibit apoptosis-related molecule expression.[42] The next study will compare the therapeutic effects of TSIIA and 3-HBA on mouse astrocytes before treatment of *A. cantonensis* L5 ESPs.

This investigation is the first to evaluate the protective function of TSIIA treatment on the central nervous system after stimulation with *A. cantonensis* L5 ESPs. These results will help develop a new therapeutic strategy for angiostrongyliasis with the possibility of clinical use in the future.

References

1. Crowe J, Lumb FE, Harnett MM, Harnett W. Parasite excretory-secretory products and their effects on metabolic syndrome. *Parasite Immunol* 2017;**39**.
2. Dzik JM. Molecules released by helminth parasites involved in host colonization. *Acta Biochim Pol* 2006;**53**:33—64.
3. Fang W, Xu S, Wang Y, Ni F, Zhang S, Liu J, et al. ES proteins analysis of *Angiostrongylus cantonensis*: products of the potential parasitism genes? *Parasitol Res* 2010;**106**:1027—32.
4. Morassutti AL, Graeff-Teixeira C. Interface molecules of *Angiostrongylus cantonensis*: their role in parasite survival and modulation of host defenses. *Int J Inflamm* 2012;**2012**:512097.
5. Bai X, Wu X, Wang X, Guan Z, Gao F, Yu J, et al. Regulation of cytokine expression in murine macrophages stimulated by excretory/secretory products from *Trichinella spiralis* in vitro. *Mol Cell Biochem* 2012;**360**:79—88.
6. Chen KY, Chiu CH, Wang LC. Anti-apoptotic effects of Sonic hedgehog signalling through oxidative stress reduction in astrocytes co-cultured with excretory-secretory products of larval *Angiostrongylus cantonensis*. *Sci Rep* 2017;**7**:41574.
7. Chen KY, Lu PJ, Cheng CJ, Jhan KY, Yeh SC, Wang L. Proteomic analysis of excretory-secretory products from young adults of *Angiostrongylus cantonensis*. *Mem Inst Oswaldo Cruz* 2019;**114**:e180556.
8. Wang LC, Jung SM, Chen KY, Wang TY, Li CH. Temporal-spatial pathological changes in the brains of permissive and non-permissive hosts experimentally infected with *Angiostrongylus cantonensis*. *Exp Parasitol* 2015;**157**:177—84.
9. Alicata JE. Present status of *Angiostrongylus cantonensis* infection in man and animals in the tropic. *J Trop Med Hyg* 1969;**72**:53—63.
10. Hochberg NS, Park SY, Blackburn BG, Sejvar JJ, Gaynor K, Chung H, et al. Distribution of eosinophilic meningitis cases attributable to *Angiostrongylus cantonensis*. *Hawaii*. *Emerg Infect Dis* 2007;**13**:1675—80.
11. Wang QP, Lai DH, Zhu XQ, Chen XG, Lun ZR. Human angiostrongyliasis. *Lancet Infect Dis* 2008;**8**:621—30.
12. Ba Z, Shi S, Huang N, Li Y, Huang J, You C, et al. Mesenchymal stem cells after the proprocessing of tanshinone IIA attenuate cognitive deficits and oxidative stress injury in an amyloid β-peptide (25-35)-induced rodent model of Alzheimer's disease. *Neuroreport* 2022;**33**:61—71.
13. Geng L, Liu W, Chen Y. Tanshinone IIA attenuates Aβ-induced neurotoxicity by down-regulating COX-2 expression and PGE2 synthesis via inactivation of NF-κB pathway in SH-SY5Y cells. *J Biol Res* 2019;**26**:15.
14. Ma HH, Wan C, Zhang LD, Zhang RR, Peng D, Qiao LJ, et al. Sodium tanshinone IIA sulfonate improves cognitive impairment via regulating Aβ transportation in AD transgenic mouse model. *Metab Brain Dis* 2022;**37**:989—1001.
15. Peng X, Chen L, Wang Z, He Y, Ruganzu JB, Guo H, et al. Tanshinone IIA regulates glycogen synthase kinase-3β-related signaling pathway and ameliorates memory impairment in APP/PS1 transgenic mice. *Eur J Pharmacol* 2022;**918**:174772.
16. Chen Y, Wu X, Yu S, Lin X, Wu J, Li L, et al. Neuroprotection of tanshinone IIA against cerebral ischemia/reperfusion injury through inhibition of macrophage migration inhibitory factor in rats. *PLoS One* 2012;**7**:e40165.
17. Dong K, Xu W, Yang J, Qiao H, Wu L. Neuroprotective effects of Tanshinone IIA on permanent focal cerebral ischemia in mice. *Phytother Res* 2009;**23**:608—13.
18. Li H, Han W, Wang H, Ding F, Xiao L, Shi R, et al. Tanshinone IIA inhibits glutamate-induced oxidative toxicity through prevention of mitochondrial dysfunction and suppression of MAPK activation in SH-SY5Y human neuroblastoma cells. *Oxid Med Cell Longev* 2017;**2017**:4517486.
19. Xiong CQ, Zhou HC, Wu J, Guo NZ. The protective effects and the involved mechanisms of tanshinone IIA on sepsis-induced brain damage in mice. *Inflammation* 2019;**2**:354—64.
20. Yao NW, Lu Y, Shi LQ, Xu F, Cai XH. Neuroprotective effect of combining tanshinone IIA with low-dose methylprednisolone following acute spinal cord injury in rats. *Exp Ther Med* 2017;**13**:2193—202.
21. Yin X, Yin Y, Cao FL, Chen YF, Peng Y, Hou WG, et al. Tanshinone IIA attenuates the inflammatory response and apoptosis after traumatic injury of the spinal cord in adult rats. *PLoS One* 2012;**7**:e38381.
22. Zhou S, Chen W, Su H, Zheng X. Protective properties of tanshinone I against oxidative DNA damage and cytotoxicity. *Food Chem Toxicol* 2013;**62**:407—12.
23. Wang J, Wang X, Jiang S, Yuan S, Lin P, Zhang J, et al. Growth inhibition and induction of apoptosis and differentiation of tanshinone IIA in human glioma cells. *J Neuro Oncol* 2007;**82**:11—21.
24. Feng Y, Feng F, Zheng C, Zhou Z, Jiang M, Liu Z, et al. Tanshinone IIA attenuates demyelination and promotes remyelination in *A. cantonensis*-infected BALB/c mice. *Int J Biol Sci* 2019;**15**:2211—23.
25. Chauhan A, Tikoo A, Patel J, Abdullah AM. HIV-1 endocytosis in astrocytes: a kiss of death or survival of the fittest? *Neurosci Res* 2014;**88**:16—22.

26. Desagher S, Glowinski J, Premont J. Astrocytes protect neurons from hydrogen peroxide toxicity. *J Neurosci* 1996;**16**:2553—62.
27. Deng J, Zhang J, Gao K, Yan W, Zhou L, Jiang Y, et al. Secretomics alterations and astrocyte dysfunction in human iPSC of leukoencephalopathy with vanishing white matter. *Neurochem Res* 2022;**47**:3747—60.
28. Rothhammer V, Quintana FJ. Control of autoimmune CNS inflammation by astrocytes. *Semin Immunopathol* 2015;**37**:625—38.
29. Liu Y, Song N, Yao H, Jiang S, Wang Y, Zheng Y, et al. β-Arrestin2-biased Drd2 agonist UNC9995 alleviates astrocyte inflammatory injury via interaction between β-arrestin2 and STAT3 in mouse model of depression. *J Neuroinflammation* 2022;**19**:240.
30. Chen KY, Cheng CJ, Cheng CC, Jhan KY, Chen YJ, Wang LC. The excretory/secretory products of fifth-stage larval *Angiostrongylus cantonensis* induces autophagy via the Sonic hedgehog pathway in mouse brain astrocytes. *PLoS Neglected Trop Dis* 2020;**14**:e0008290.
31. Chen KY, Chen YJ, Cheng CJ, Jhan KY, Wang LC. Excretory/secretory products of *Angiostrongylus cantonensis* fifth-stage larvae induce endoplasmic reticulum stress via the Sonic hedgehog pathway in mouse astrocytes. *Parasites Vectors* 2020;**13**:317.
32. Chen KY, Wang LC. Stimulation of IL-1β and IL-6 through NF-κB and sonic hedgehog-dependent pathways in mouse astrocytes by excretory/secretory products of fifth-stage larval *Angiostrongylus cantonensis*. *Parasites Vectors* 2017;**10**:445.
33. Thanaviratananich S, Thanaviratananich S, Ngamjarus C. Corticosteroids for parasitic eosinophilic meningitis. *Cochrane Database Syst Rev* 2015;**2015**:CD009088.
34. Tsai HC, Lee BY, Yen CM, Wann SR, Lee SS, Chen YS, et al. Dexamethasone downregulated the expression of CSF 14-3-3β protein in mice with eosinophilic meningitis caused by *Angiostrongylus cantonensis* infection. *Acta Trop* 2014;**131**:98—103.
35. Lam HYP, Liang TR, Jiang SJ, Peng SY. Albendazole-schisandrin B Co-therapy on *Angiostrongylus cantonensis*-induced meningoencephalitis in mice. *Biomolecules* 2020;**10**:1001.
36. Feng F, Feng Y, Liu Z, Li WH, Wang WC, Wu ZD, et al. Effects of albendazole combined with TSII-A (a Chinese herb compound) on optic neuritis caused by *Angiostrongylus cantonensis* in BALB/c mice. *Parasites Vectors* 2015;**8**:606.
37. Jhan KY, Cheng CJ, Jung SM, Lai YJ, Chen KY, Wang LC. Co-therapy of albendazole and dexamethasone reduces pathological changes in the cerebral parenchyma of Th-1 and Th-2 dominant mice heavily infected with *Angiostrongylus cantonensis*: histopathological and RNA-seq analyses. *Biomolecules* 2021;**11**:536.
38. Tai H, Jiang XL, Lan ZM, Li Y, Kong L, Yao SC, et al. Tanshinone IIA combined with CsA inhibit myocardial cell apoptosis induced by renal ischemia-reperfusion injury in obese rats. *BMC Complement Med Ther* 2021;**21**:100.
39. Morotti M, Zois CE, El-Ansari R, Craze ML, Rakha EA, Fan SJ, et al. Increased expression of glutamine transporter SNAT2/SLC38A2 promotes glutamine dependence and oxidative stress resistance, and is associated with worse prognosis in triple-negative breast cancer. *Br J Cancer* 2021;**124**:494—505.
40. Park MW, Cha HW, Kim J, Kim JH, Yang H, Yoon S, et al. NOX4 promotes ferroptosis of astrocytes by oxidative stress-induced lipid peroxidation via the impairment of mitochondrial metabolism in Alzheimer's diseases. *Redox Biol* 2021;**41**:101947.
41. Chen R, Chen W, Huang X, Rui Q. Tanshinone IIA attenuates heart failure via inhibiting oxidative stress in myocardial infarction rats. *Mol Med Rep* 2021;**23**:404.
42. Chen KY, Chen YJ, Cheng CJ, Jhan KY, Chiu CH, Wang LC. 3-Hydroxybenzaldehyde and 4-Hydroxybenzaldehyde enhance survival of mouse astrocytes treated with *Angiostrongylus cantonensis* young adults excretory/secretory products. *Biomed J* 2021;**44**:S258—66.